



Multi-points 3D Stretch-Press-Bending Process for Forming of W-Shaped Mirror-Symmetrical Structural Parts

Song Gao¹ · Yingli Sun¹ · Qihan Li¹ · Tonggui He¹ · Jicai Liang²

Received: 17 October 2020 / Revised: 3 September 2021 / Accepted: 10 November 2021 / Published online: 11 February 2022
© Korean Society for Precision Engineering 2022

Abstract

To improve the aerodynamic performance of high-end equipment, the mirror-symmetrically 3D curved aluminum structural parts are increasingly assembled in the manufacturing industry. A new type of multi-points 3D stretch-press-bending (3D SPB) process for forming this kind of component is proposed in this paper. A prototype of this process is developed. The 3D SPB experiments are carried out. This new process realizes the complex bending for multi-directional curvature radius, which increases the material utilization by 6.79% and doubles the production efficiency. Then, the numerical simulation models are established. It has a good prediction result for the 3D springback. The maximum relative error of springback prediction is less than 20%. Besides, the effect of pre-stretching and post-stretching are investigated, which determines the most suitable forming parameters at ϵ_s pre-stretching and $0.3 \epsilon_s$ post-stretching. At last, the springback direct compensation method is applied to the precise forming of the target part. Though two times adjustment, the deviation reduces effectively. The precise forming experiment is carried out based on the optimized forming parameters. The maximum total deviation is 1.52 mm, which satisfies the forming requirement. The 3D SPB process achieves the pairwise forming of the W-shaped mirror-symmetric structural parts and improves production efficiency.

Keywords Multi-points forming · Stretch-bending · Springback · Precise forming

1 Introduction

Aluminum extrusion bending parts are widely used as structural components in aerospace, rail transportation, automobile and other vehicle manufacturing industries [1, 2]. The stretch-bending process is one of the primary methods for producing such parts. It has the characteristics of high forming accuracy, simplicity and excellent repeatability [3, 4]. The application of axial tensile force improves the formability of extrusion. The high-aerodynamic-performance 3D stretch-bending structural parts are more and more designed and adopted in high-end equipment [5]. As shown in Fig. 1, the window's upper and lower beams are 3D curved aluminum structural parts in the high-speed trains. They are usually used in pairs and arranged mirror-symmetrically.

The 3D stretch-bending process is the primary method to produce this kind of 3D curved parts. In this process, the extrusion is stretched and deformed along its axis, and it is bent in two planes perpendicular to its axial section [6]. The solid die or the multi-point die (MPD) is adopted in the 3D stretch-bending process. It needs artificial adjustment for the die shape before forming [7]. The clamps are used to drive the workpiece to form the target shape. Generally, for the production of the pair of mirror-symmetrical parts, as shown in Fig. 1, each single geometrically asymmetrical part is formed separately with different sets of tools. If the two mirror-symmetrical parts can be formed simultaneously, the processing efficiency can be doubled. However, due to the forming tool's limitation, the extrusion can only be bent in one radius of curvature on each plane in the conventional forming process [8]. Besides, after forming, it is necessary to manually correct the workpiece's geometry shape or adjust the die shape because of the springback problem [9–11].

In view of the production situation of the 3D stretch-bending parts, a new type of multi-points 3D stretch-press-bending process (3D SPB) is proposed in this work. A prototype of this forming equipment is developed. This method

✉ Song Gao
gaosong@ccut.edu.cn

¹ School of Mechatronic Engineering, Changchun University of Technology, Changchun 130012, Jilin, China

² College of Material Science and Engineering, Jilin University, Changchun 130022, Jilin, China

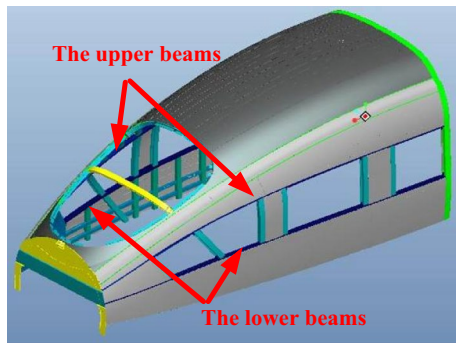


Fig. 1 The skeleton of high-speed train

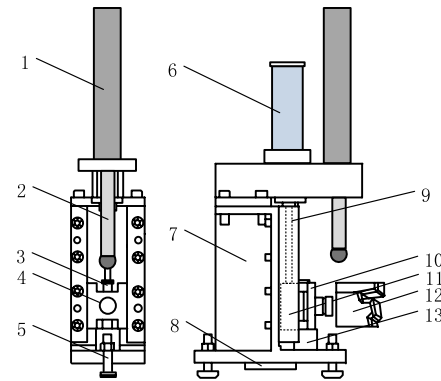
realizes the complex bending for multi-directional curvature radius, such as the 3D "W" shaped bending. Based on this new forming technology, the pair of lower beams on the high-speed train in Fig. 1 are precisely formed.

2 The Multi-points 3D Stretch-Press-Bending Process

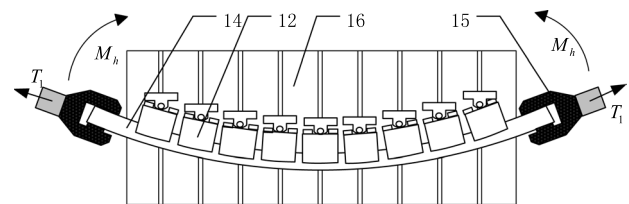
The 3D SPB process is developed based on the flexible 3D stretch-bending process (3D FSB) [6, 7]. By using the movable MPD, the workpiece can be 3D superposition deformed. In order to achieve the complex 3D "W" shaped stretch-bending, a hydraulic press cylinder is installed at the end of each flexible fundamental unit (FFU) to press and bend the workpiece on the horizontal curved surface. In the 3D SPB process, the horizontal bending is performed by clamps, while the hydraulic actuators perform the vertical bending on each FFU. The forming principle is shown in Fig. 2.

The structure of the FFU is shown in Fig. 2a. As the carrier of the MPD, it plays an essential role in forming a "W" curved part. It comprises a press bending cylinder, a reset air cylinder, MPD, a bracket, a backplane, and other components. The workpiece will be pressed to the vertical target shape on the curved surface. The multi-directional curvature radii can be formed by control the downward displacement of each piston rod, as shown in Fig. 2c. Besides, the reset air cylinder is also newly added to reset the MPD to the initial position. The newly added actuators realize the complex bending and reduce the labour intensity. They also help to improve the forming accuracy and production efficiency.

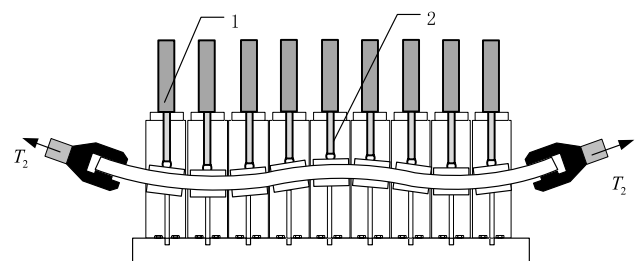
A prototype of 3D SPB forming equipment is developed, as shown in Fig. 3, including the FFU group, MPD, 3D bending manipulator, and control station. The forming process includes four procedures, which are summarized as follows:



(a) The structure of FFU in 3D SPB



(b) The horizontal bending



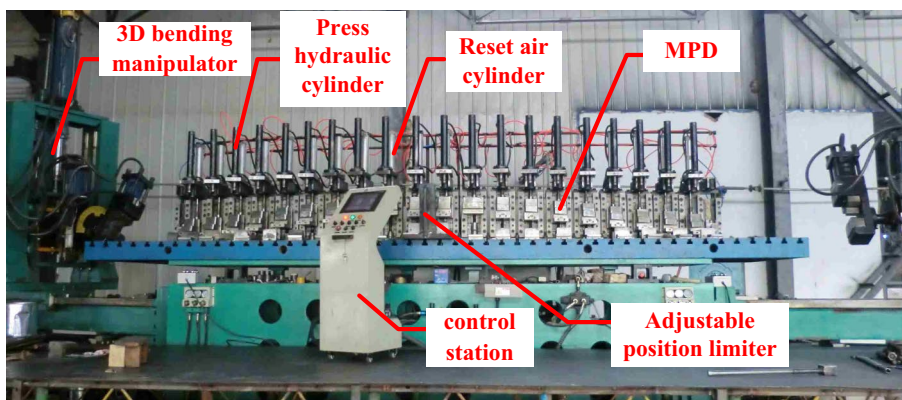
(c) The vertical bending

1-Press bending cylinder; 2-Piston rod; 3-Vertical pin; 4-Horizontal pin; 5-Bolt; 6-Reset air cylinder; 7-Bracket; 8-Guide key; 9-Cylinder rod; 10- Backplane; 11- Guide slider; 12-MPD; 13- Stop block; 14-Workpiece; 15-Clamp; 16-Workbench;

Fig. 2 The forming principle of 3D SPB

- 1) At first, the enveloping shape of the MPD group is adjusted to the target geometry in the horizontal direction, and the vertical position is reset on the same height position. The clamps fix the workpiece at both ends, and it is pre-stretched to the initial yield stress.
- 2) As shown in Fig. 2b, the clamps drive the workpiece to bend in the horizontal direction.
- 3) As shown in Fig. 2c, once the clamps reach the specified position, the press hydraulic cylinder acts on each FFU making the MPD move downward in the vertical direction, which realizes vertical bending.
- 4) A post-stretch procedure is applied to improve the forming accuracy and reduce springback.

Fig. 3 The 3D SPB forming equipment prototype



3 Pair Forming of the Lower Beams for High-Speed Trains

Take the pair of lower beams in Fig. 1 as the target parts, and the experiments are carried out based on the 3D SPB equipment. The geometry shape of the mirror-symmetrical lower beams is shown in Fig. 4. It utilizes the AA6061 aluminum extrusion with a T-shaped cross-section. The cross-section is shown in Fig. 4a. The W-shaped workpiece is bent and deformed on two orthogonal planes, demonstrated in Fig. 4b, c. The final length of a single part is 2100 mm, drawn with solid black lines. Since the connection places will generate considerable strain and stress concentration, it needs to reserve removal margins at both ends of the final part, which are 500 mm on the left and 600 mm on the right (marked in blue). The workpiece length is 3200 mm in the conventional 3D stretch-bending process for forming a single lower beam. The calculated material utilization rate is 65.62%. When the 3D SPB is used, the pair of mirror-symmetrical parts is produced as a whole workpiece. The non-deformed ends of the pair of parts are connected, so the 600 mm removal margin in the middle section of the profile can be reduced. The workpiece length is 3200 mm + 2100 mm + 500 mm = 5800 mm, and the material utilization rate is 72.41%, effectively

reducing the manufacturing cost and doubles the production efficiency.

There are 20 FFU used in the forming of the pair of lower beams. The width of the MPD is 115 mm, and the interval is 238.25 mm. Take the shape of the target part as the envelope surface to adjust the MPD on each FFU. Based on the 3D SPB equipment, different forming steps are shown in Fig. 5. Under the displacement control method, the workpiece was installed through the adjustable position limiter and pre-stretched to the initial yield stress (Fig. 5a). Then, as shown in Fig. 5b, c, it was bent and pressed in the horizontal and vertical directions. The final forming part is shown in Fig. 5d. The shape in the vertical direction forms a “W” shape with multi-directional curvatures.

The 3D SPB process successfully achieved the pair forming of the mirror-symmetrical lower beams while improving the material utilization rate by 6.79% and increasing the production efficiency by double. By observing the appearance of the formed part, there are no wrinkles and cross-sectional deformation occurred. To quantitatively represent the geometric shape of the formed part, the characteristic curves between the target shape and the formed shape is shown in Fig. 6a. The shape of the formed part is consistent with the shape of the target part. Besides, no sharp local bending defects and irregular deformation occurred along the axial direction of the profile. However, the target and

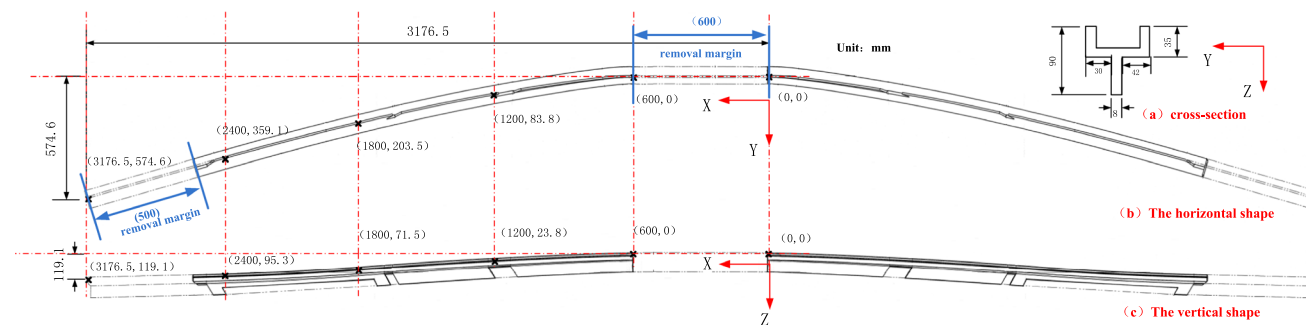


Fig. 4 The geometry shape of the W-shape workpiece and the lower beams

Fig. 5 The 3D SPB process for forming of the pair of lower beams

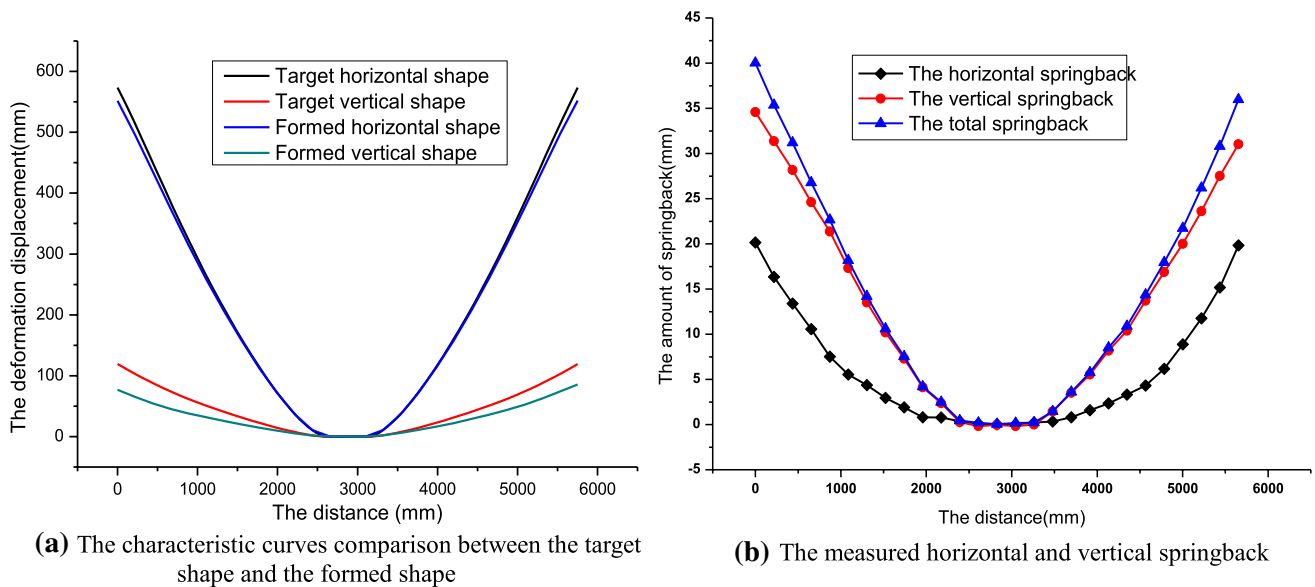
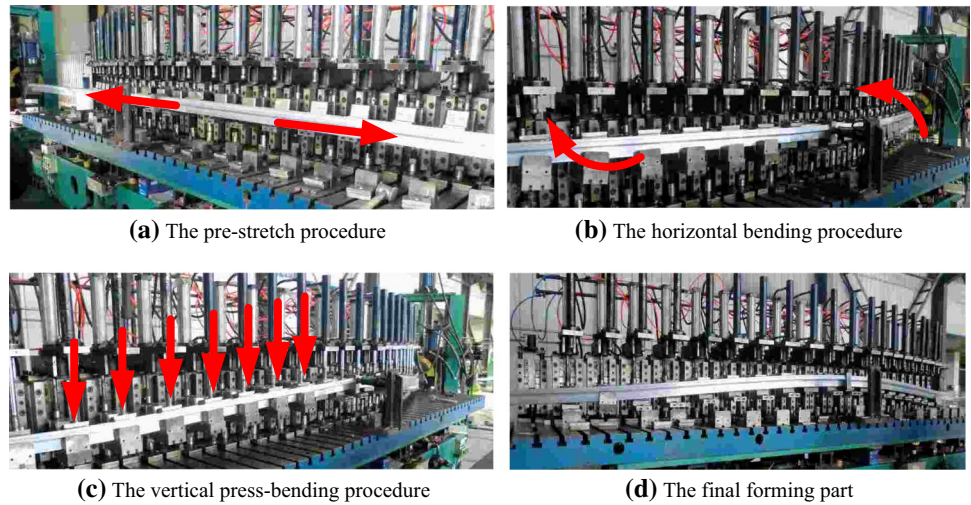


Fig. 6 The measured 3D springback curves

formed curves do not overlap because of springback. Take the deformation deviation of contour in the horizontal and vertical directions to quantify the 3D springback[12]. The measured springback curves are shown in Fig. 6b. The distance is the displacement from one end to the other end of the workpiece in the X-axis. The total springback is the linear distance before and after springback deformation at the measuring point. It can be divided into horizontal and vertical springback. Since vertical bending plays a post-stretching effect on horizontal bending, the springback in the horizontal direction is smaller than that in the vertical direction. The maximum horizontal springback is 21.15 mm, while the maximum vertical springback is 34.58 mm. Such a large springback deformation seriously affects the forming accuracy.

4 Numerical Simulation of the 3D SPB Process

In order to realize the effective control of springback, the method of numerical simulation is used to study the 3D SPB forming process and springback deformation process for the target parts.

4.1 Material Model

The mechanical property of AA6061-T6 aluminum alloy is measured by the uniaxial tensile test. The size of a standard sample with a material thickness of 2 mm is shown

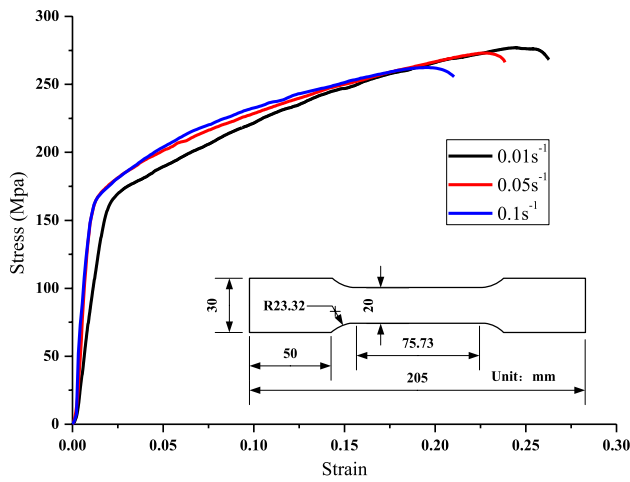


Fig. 7 The stress-strain curves of AA6061

in Fig. 7. The true stress–strain curves at room temperature with strain rates of 0.01 s^{-1} , 0.05 s^{-1} , and 0.1 s^{-1} were measured on an electronic universal tensile testing machine (maximum tensile force is 100 kN).

The material of AA6061 has stable properties at room temperature. The change of strain rate affects the tensile strength, but it barely affects the yield stress. Its value keeps at 168 MPa. The elastic modulus of the AA6061 is 68.9 GPa. As the strain rate decreases, the material's ductility increases, and the tensile strength reaches a higher value. According to the actual forming conditions of the 3D SPB process, the Hollomon model (Eq. 1) [13], Voce model (Eq. 2) [14], and Swift model (Eq. 3) [15] were used to establish the constitutive flow relationship at 0.05 s^{-1} strain rate.

$$\sigma = K\varepsilon^{n_1} \tag{1}$$

$$\sigma = \sigma_s + Z(1 - e^{-m\varepsilon}) \tag{2}$$

$$\sigma = D(\varepsilon + \varepsilon_s)^k \tag{3}$$

where K is the strength factor, σ_s is yield stress, n_1, Z, m, D are the material parameters, they are calculated and fitted in Table 1.

As shown in Fig. 8, the established constitutive equations are compared with the experiment data. It can be seen that the three constitutive models can adequately describe the flow hardening law of AA6061. However, after entering the initial yield state, the Swift constitutive model can better fit the test data curve, while the other two models have significant errors. Therefore, in this simulation, it is assumed that the mechanical properties of aluminum extrusions follow the Mises yield criterion and the Swift flow rule. It is isotropic in elastoplastic constitutive behavior.

Table 1 The material parameters

Material parameter	Value
$K/(\text{MPa})$	384
$\sigma_s/(\text{MPa})$	175
n_1	0.35
$Z/(\text{MPa})$	203
m	2.99
$D/(\text{MPa})$	382
k	0.24
ε_s	0.002438

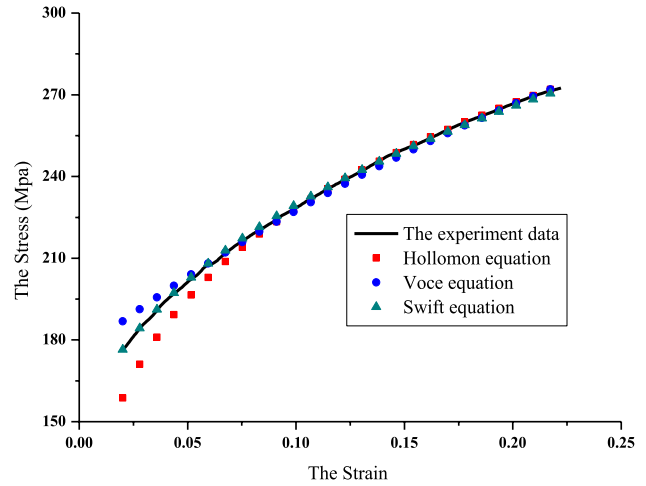


Fig. 8 Constitutive model curves

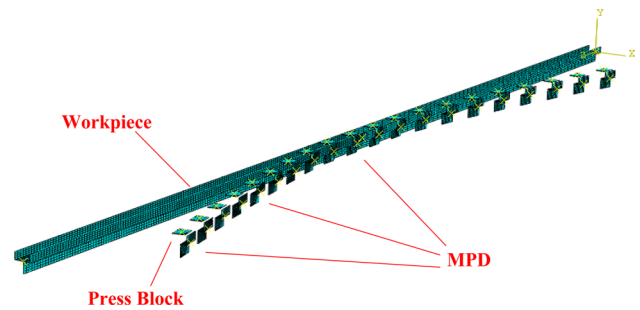


Fig. 9 The finite element model

4.2 Finite Element Model

According to the 3D SPB forming process for the lower beams in Sect. 3, the finite element model was established using ABAQUS [16], as shown in Fig. 9. The geometry shape and the boundary conditions are the same as the experimental forming parameters. Since the cross-section thickness is uniform, the shell element S4R is used to mesh the workpiece. Assuming that the MPD does not deform during the forming process, the rigid element R3D4 is adopted.

The clamps are abstracted as reference points at the two ends of the workpiece. The displacement is loaded on two points to drive the workpiece to form in the horizontal direction. On the vertical plane, the press bending cylinder is simplified as a pressing block. By controlling the displacement of each press block, the W-shaped bending can be realized.

4.3 Simulation Results

The simulation results using the ABAQUS/Explicit dynamic algorithm are demonstrated in Fig. 10. There are no cracks, no sharp local bending defect, and no wrinkles on the formed part. The forming part has a uniform stress distribution. The stress distribution after the pre-stretching is shown in Fig. 10a. The maximum stress and equivalent plastic strain are 177.12 MPa and 0.00106, bringing the workpiece to a yielding state. In Fig. 10b, the workpiece is bent in the horizontal plane, the maximum stress and equivalent plastic strain reach 206.98 MPa and 0.04446. The stress concentration appears in some stretched areas on the outside of the workpiece. This situation has been improved after the vertical bending procedure. As shown in Fig. 10c, the stress is released, and the maximum value is reduced to 199.43 MPa. Meanwhile, the equivalent plastic strain continues to increase to 0.06742. The simulation shape of the workpiece is consistent with the actual experimental result. The workpiece is deformed to the 3D W-shape part as the target shape of the lower beams.

Based on the forming simulation results, a springback model for the formed part is established. The ABAQUS/Standard static implicit algorithm is used to predict the springback deformation. The simulation results are shown in Fig. 11. The $\Delta\alpha_y$ and $\Delta\alpha_z$ represent the springback deviation in the horizontal and vertical directions. The maximum values appear at both ends of the workpiece, 21.84 mm and 42.03 mm for $\Delta\alpha_y$ and $\Delta\alpha_z$. The total springback $\Delta\alpha = \sqrt{\Delta\alpha_y^2 + \Delta\alpha_z^2}$ at the maximum point is 47.37 mm. The maximum residual stress after springback deformation is reduced to 89.52 MPa.

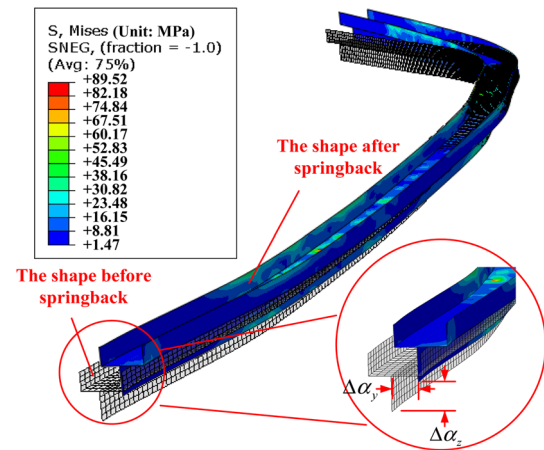
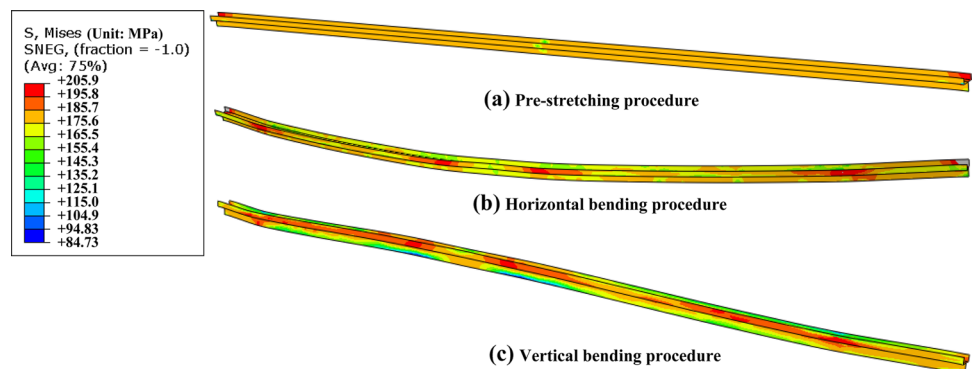


Fig. 11 The springback simulation results

The simulation result is compared with the experimental formed parts in Fig. 12. After springback, they have the same geometry characteristic. The springback of the simulation result is shown in Fig. 13. The horizontal springback is also smaller than the vertical springback. The amount of springback on the left and right sides in the horizontal direction is nearly the same. However, a severe imbalance occurs in the vertical direction. The clamps on both sides are loaded synchronously during the forming process, and symmetrical and equal boundary conditions are used. The reason for this phenomenon is that the deformation in the vertical direction is small, so the unevenness of deformation exists in the process of vertical bending. Due to the uneven distribution of residual stress, the springback on these two sides is significantly different. When the post-stretching is applied, this phenomenon will be reduced or even disappear.

As shown in Fig. 14a, the prediction error of simulation result in the horizontal direction is always less than 2 mm on the entire profile, but a large error occurs in the vertical direction, especially on the left side of the formed part. The maximum prediction error reached 7.45 mm. The absolute error of springback prediction is converted to the relative error, shown in Fig. 14b. The absolute error is the difference

Fig. 10 The simulation results of the 3D SPB process



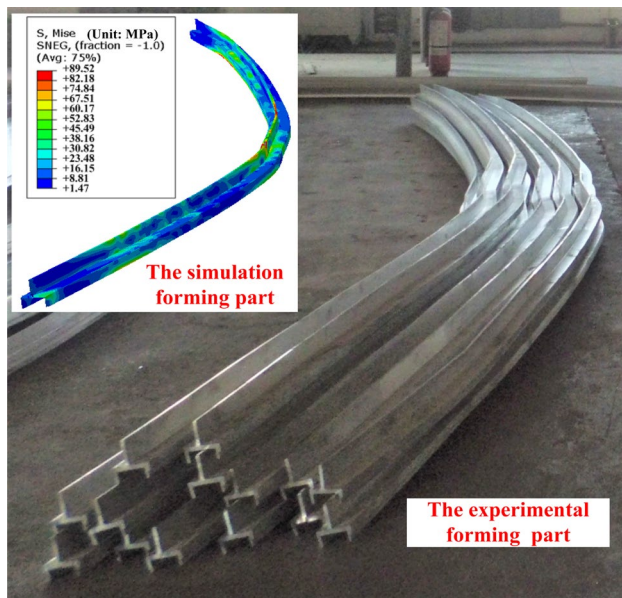


Fig. 12 The comparison between the experiment and the simulation after springback

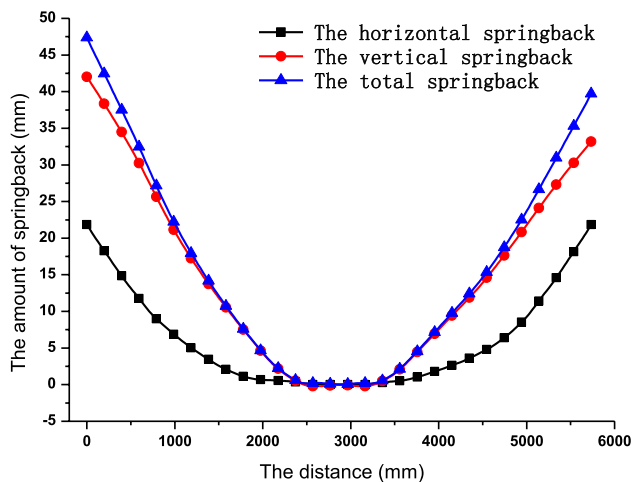


Fig. 13 The simulation springback curves

between the predicted springback by simulation and the experimentally measured springback. The relative error is the absolute error divided by the experimental springback value, representing a relative value of prediction accuracy. It can be seen that the maximum relative error of springback prediction is 19.89% appeared in the middle of the workpiece, which is because the deformation of the intermediate position itself is minimal. The relative error in the area with large deformation is less than 16% without considering the middle position. The above analysis shows that the numerical simulation model has a good prediction result for the 3D springback of the 3D SPB forming part. It effectively

predicts the changing trend of springback deformation in the entire length of the workpiece, which is in good agreement with the experimental data.

5 Precise Forming of the Lower Beams

The method of controlling the springback deformation is studied from two aspects in this section. One is to reduce the springback by changing the axial tensile state; the other is to control the springback by the springback compensation method.

5.1 Effects of the Tension

It is well known that the axial tension can reduce springback and improve forming accuracy in the stretch-bending process. However, excessive tension will destroy the cross-sectional shape [17]. Based on the established simulation model, the effect of pre-stretching and post-stretching on springback in the 3D SPB process is firstly investigated.

5.1.1 Pre-stretching

Under no post-stretching condition, the different pre-stretching strain states $0, 0.5 \epsilon_s, \epsilon_s, 1.5 \epsilon_s$, was applied to study the effect of pre-stretching on the springback deformation, where ϵ_s is the yield strain of the material. Figure 15 demonstrates the relationship between springback and the change of pre-stretching state. As shown in Fig. 15a, as the pre-stretching strain increases from zero to the yield strain ϵ_s , the maximum horizontal springback decreases by 42.43%. Then it becomes stable when the pre-stretching strain exceeds ϵ_s . The springback in the vertical direction presents a more severe asymmetry in Fig. 15b. With the increase of pre-stretching, the vertical springback has a trend of increasing on the left and decreasing on the right, meanwhile, the total springback shows a downward trend in Fig. 15c. The curve of the maximum springback vs the pre-stretching state is shown in Fig. 15d. It can be seen that pre-stretching can reduce the springback deformation, but the effect is not apparent after its value exceed ϵ_s . In the case of ϵ_s and $1.5 \epsilon_s$, the forming process is carried out entirely in the plastic state, the springback deformation is the same, but in the case of $1.5 \epsilon_s$, the deformation of the section is more serious. According to the analysis above, the pre-stretching strain set as ϵ_s is the most suitable value for the 3D SPB process.

5.1.2 Post-stretching

Under the ϵ_s pre-stretching strain condition, the different post-stretching states at $0, 0.3 \epsilon_s, 0.6 \epsilon_s, 0.9 \epsilon_s$ are adopted to research its effect on springback. The relationship between

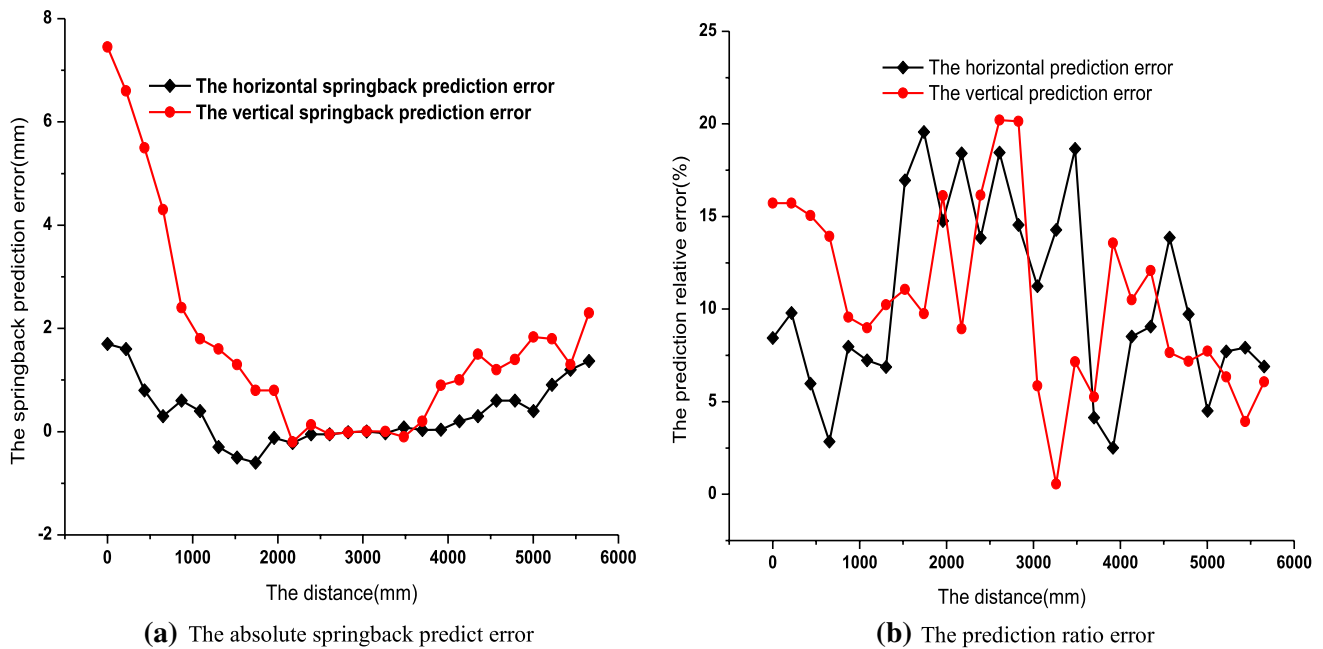


Fig. 14 The springback predict error

springback and the post-stretching state is shown in Fig. 16. The application of post-stretching tension significantly reduces the amount of springback. When the post-stretching increased from 0 to $0.3 \varepsilon_s$, as shown in Fig. 16a–c, the springback decreased by 55.33% and 91.27% in the horizontal and vertical directions. The total springback decreased by 77.64%. The horizontal springback drops to 9.94 mm, and the vertical springback reduces to 3.67 mm. Besides, the application of post-stretching offsets residual stress so that the springback at both ends of the workpiece becomes symmetric and uniform. However, during the process of increasing the post-stretching state from $0.3 \varepsilon_s$ to $0.9 \varepsilon_s$, the springback deformation tends to be stable, and no further reduction is reached, as shown in Fig. 16d, the maximum total springback is only reduced by 5.12%, but the probability of defects such as deformities, fractures and wall thickness reduction is increased. We can conclude that the post-stretching effect significantly reduces springback, especially for the vertical springback in the 3D SPB process. The $0.3 \varepsilon_s$ post-stretching state is a suitable value to produce this part. Since the forming requirement of this part is that the maximum total deviation should be less than 2 mm, it needs further control of the forming accuracy.

5.2 The Springback Compensation

In order to further control the springback, the direct compensation method was adopted to adjust the envelope

surface of the MPD [18]. The direct compensation method uses the measured springback error as the over-adjust displacement for each MPD position parameter to compensate the springback. In the previous analysis, the initial envelop surface of MPD is the shape of the target part. The springback errors obtained by the simulation in the case of ε_s pre-stretching and $0.3 \varepsilon_s$ post-stretching are used to compensate for the original envelope surface. The iterative compensated envelop surface can be expressed as:

$$E^{j+1} = E^j + a\Delta\alpha^j \quad (4)$$

where E represents the shape of envelope surface formed by the MPD, it equal to the shape of target part at initial adjustment, j is the number of iterations, a is the compensation factor equal to -1 in this work. After the two times iteration, the envelop surfaces of MPD are presented in Fig. 17, in which Fig. 17a is the change of horizontal envelop surface, Fig. 17b is the change of vertical envelop surface. The simulation results of the springback are shown in Fig. 17c–e. The deviation is defined as the displacement from the simulated formed shape to the target shape. The maximum horizontal deviation is reduced from 9.94 mm to 1.38 mm, and the maximum vertical deviation is reduced from 3.67 mm to 0.65 mm. The maximum total deviation is 1.50 mm after the second adjustment, which dropped by 85.84% and met the requirements of forming accuracy. Therefore, it can be concluded that the precision forming of the target part is achieved by using the direct compensation method.

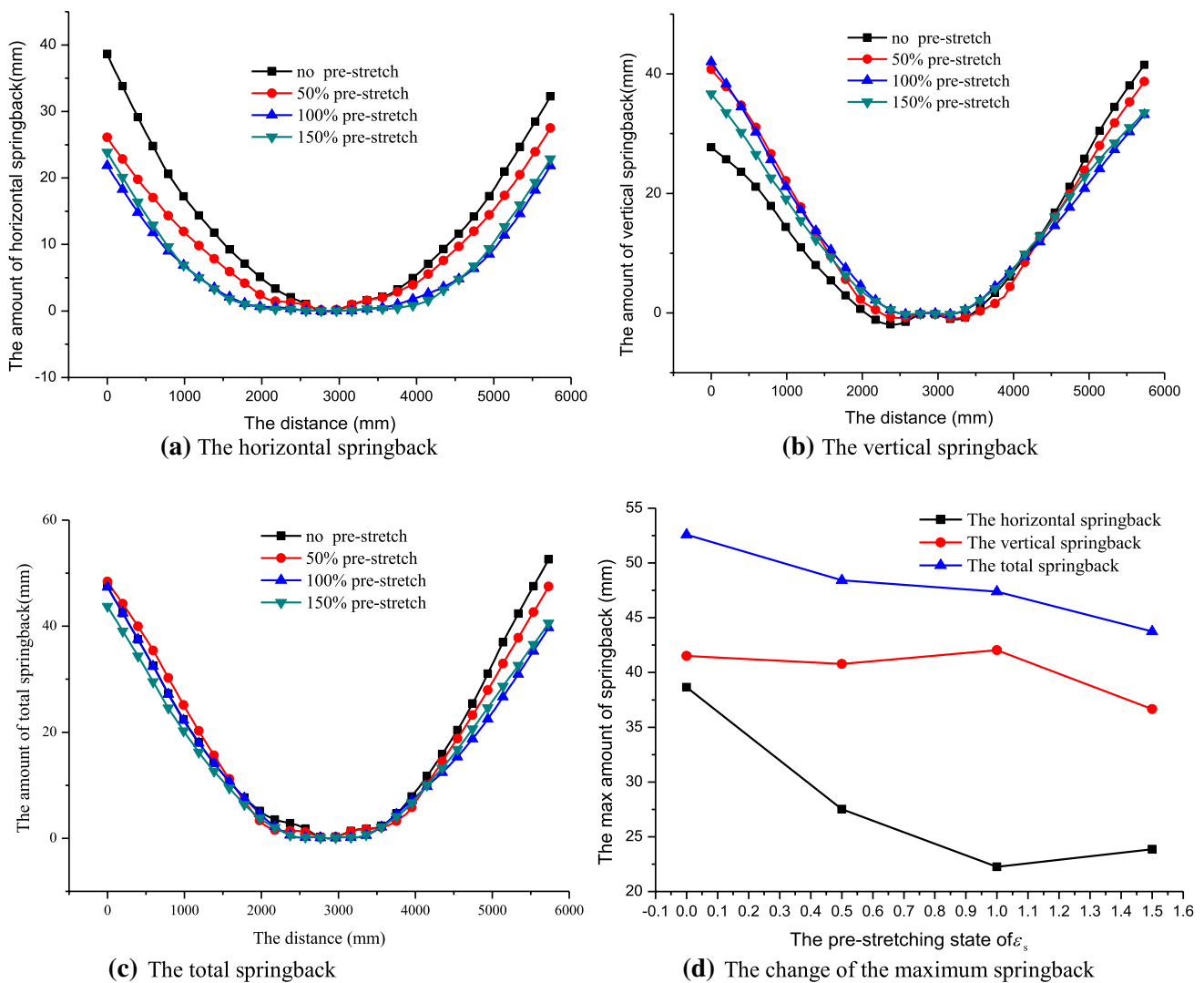


Fig. 15 The effect of the pre-stretching state

5.3 Precise Forming Experiment

According to the above analysis, the 3D SPB experiment is carried out based on the optimized forming process parameters. They are ϵ_s pre-stretching, $0.3 \epsilon_s$ post-stretching, and the adjustment parameters after compensation. The deviation of the experiment result is shown in Fig. 18. The maximum deviation is 1.33 mm in the horizontal direction and 0.73 mm in the vertical direction. The maximum total deviation is 1.52 mm, which also satisfies the forming requirement. The final forming parts with the springback detection tools are shown in Fig. 19. The workpiece has been cut to the final shape of the window’s lower beams for the high-speed trains. The test results verify the effectiveness of analyzed process parameters and achieve the precise forming of the W-shaped mirror-symmetrical structural parts.

6 Conclusions

A new type of multi-points 3D stretch-press-bending process for forming W-shaped mirror-symmetrical aluminum structural parts is proposed in this paper. A prototype of this forming equipment is developed. This method realizes the complex bending for multi-directional curvature radius, such as the 3D "W" shaped bending. It also achieves the pairwise forming of mirror-symmetric structural parts and improves production efficiency. The conclusions are as follows.

Compared with the conventional process, the new process improves the material utilization rate by 6.79%, effectively reducing manufacturing costs and doubles production efficiency.

The numerical simulation model has a good prediction result for the 3D springback of the 3D SPB forming part. The maximum relative error of springback prediction in

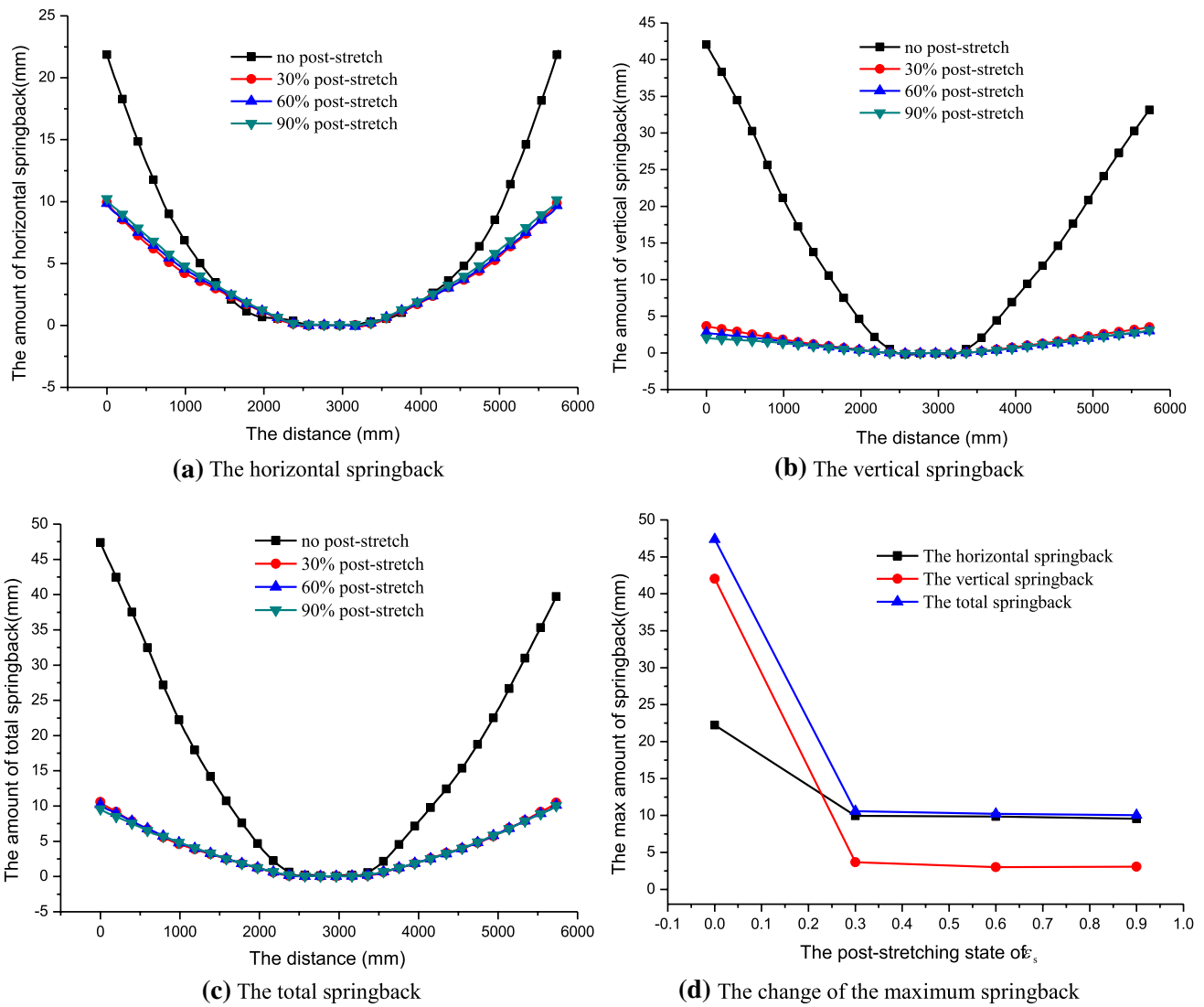


Fig. 16 The effect of the post-stretching state

horizontal and vertical directions is less than 20%. It effectively predicts the changing trend of the springback deformation in the entire length of the workpiece.

The pre-stretching and post-stretching both affect to reduce the springback. Especially, the post-stretching has the effect of significantly reducing the vertical springback. The $1 \epsilon_s$ pre-stretching and $0.3 \epsilon_s$ post-stretching parameters are considered as the most suitable value to manufacturing mirror-symmetrical parts.

At last, the direct springback compensation method is applied to the precise forming of the target part. Though two times compensation of the envelope surface, the maximum total deviation reduces from 10.59 mm to 1.50 mm, which dropped by 85.84%. The precise forming experiment is carried out based on the optimized forming process parameters. The maximum total deviation is 1.52 mm, which satisfies the forming requirement. The test results verify the effectiveness of the analyzed process parameters and achieve the precise forming of the W-shaped mirror-symmetrical structural parts.

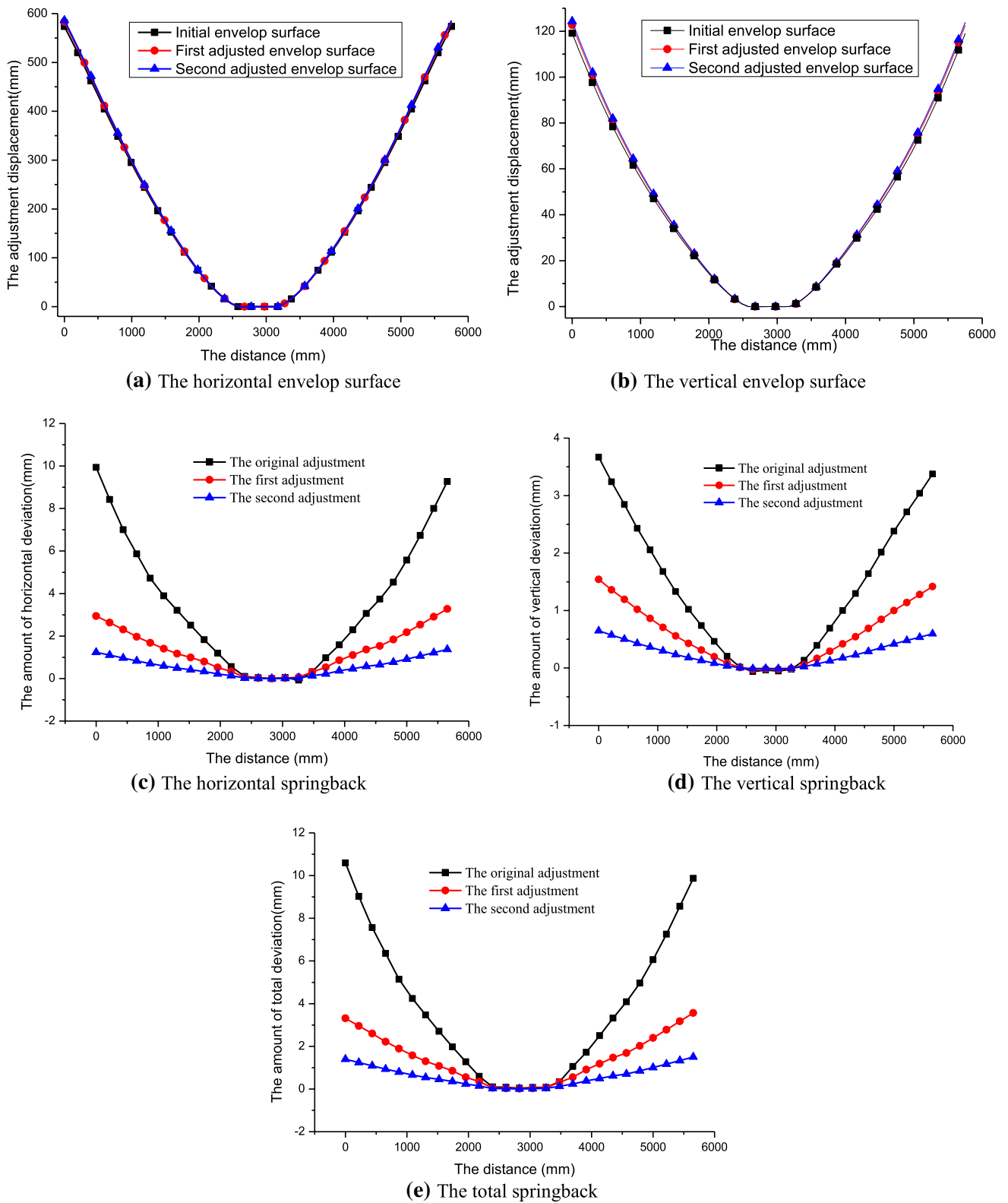


Fig. 17 The springback compensation results

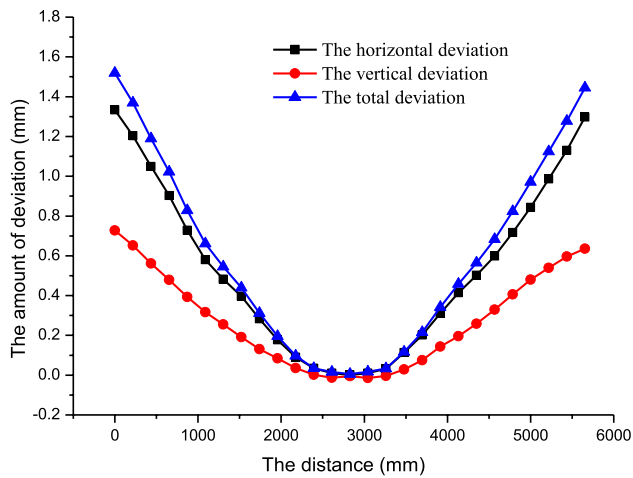


Fig. 18 The experiment results

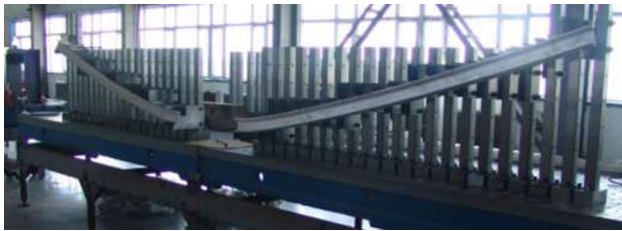


Fig. 19 The precise forming part

Acknowledgements This work was supported by the National Natural Science Foundation of China (No.51805045) and Scientific and Technological Developing Scheme of Ji Lin Province (No. 20200401115GX)

Declaration

Conflict of interest The authors declare that they have no known competing financial interests or personal relationships that could have appeared to influence the work reported in this paper.

References

- Vollertsen, F., Sprenger, A., Kraus, J., & Arnet, H. (1999). Extrusion, channel, and profile bending: A review. *Journal of Materials Processing Technology*, 87(1–3), 1–27. [https://doi.org/10.1016/S0924-0136\(98\)00339-2](https://doi.org/10.1016/S0924-0136(98)00339-2)
- Xunzhong, G., Hao, X., Heng, L., Yong, X., Ziqi, M., Abd, E. A. A., et al. (2018). Forming characteristics of tube free-bending with small bending radii based on a new spherical connection. *International Journal of Machine Tools and Manufacture*, 133, 72–84.
- Miller, J. E., Kyriakides, S., & Bastard, A. H. (2001). On bend-stretch forming of aluminum extruded tubes—I: Experiments. *International Journal of Mechanical Sciences*, 43(5), 1283–1317. [https://doi.org/10.1016/S0020-7403\(00\)00039-4](https://doi.org/10.1016/S0020-7403(00)00039-4)
- Liu, T. J., Wang, Y. J., Wu, J. J., Xia, X. J., Wang, J. B., Wang, W., & Wang, S. H. (2015). Springback analysis of Z & T-section 2196–T8511 and 2099–T83 Al-Li alloys extrusions in displacement controlled cold stretch bending. *Journal of Materials Processing Technology*, 225, 295–309. <https://doi.org/10.1016/j.jmatprotec.2015.05.024>
- Chatti, S., Hermes, M., Tekkaya, A. E., & Kleiner, M. (2010). The new TSS bending process: 3D bending of profiles with arbitrary cross-sections. *CIRP Annals—Manufacturing Technology*, 59(1), 315–318. <https://doi.org/10.1016/j.cirp.2010.03.017>
- Liang, J.-c., Gao, S., Teng, F., Yu, P.-z., & Song, X.-j. (2014). Flexible 3D stretch-bending technology for aluminum profile. *International Journal of Advanced Manufacturing Technology*, 71(9–12), 1939–1947. <https://doi.org/10.1007/s00170-013-5590-9>
- Gao, S., Liang, J. C., Li, Y., Hao, Z. P., Li, Q. H., Fan, Y. H., & Sun, Y. L. (2018). Precision forming of the 3D curved structure parts in flexible multi-points 3D stretch-bending process. *The International Journal of Advanced Manufacturing Technology*, 95(1–4), 1205–1213. <https://doi.org/10.1007/s00170-017-1276-z>
- Corona, E. (2004). Simple analysis for bend-stretch forming of aluminum extrusions. *International Journal of Mechanical Sciences*, 46(3), 433–448. <https://doi.org/10.1016/j.ijmecsci.2004.03.010>
- Clausen, A. H., Hopperstad, O. S., & Langseth, M. (2001). Sensitivity of model parameters in stretch bending of aluminium extrusions. *International Journal of Mechanical Sciences*, 43(2), 427–453. [https://doi.org/10.1016/S0020-7403\(00\)00012-6](https://doi.org/10.1016/S0020-7403(00)00012-6)
- Wagoner, R. H., Lim, H., & Lee, M.-G. (2013). Advanced Issues in springback. *International Journal of Plasticity*, 45, 3–20. <https://doi.org/10.1016/j.ijplas.2012.08.006>
- Elsharkawy, A. A., & El-Domiati, A. A. (2001). Determination of stretch-bendability limits and springback for T-section beams. *Journal of Materials Processing Technology*, 110(3), 265–276. [https://doi.org/10.1016/S0924-0136\(00\)00885-2](https://doi.org/10.1016/S0924-0136(00)00885-2)
- Teng, F., Zhang, W., Liang, J., & Gao, S. (2015). Springback prediction and optimization of variable stretch force trajectory in three-dimensional stretch bending process. *Chinese Journal of Mechanical Engineering*, 28(6), 1132–1140.
- Yu, C. L., & Li, X. Q. (2011). Theoretical analysis on springback of L-section extrusion in rotary stretch bending process. *Transactions of the Nonferrous Metals Society of China*, 21(12), 2705–2710. [https://doi.org/10.1016/S1003-6326\(11\)61113-8](https://doi.org/10.1016/S1003-6326(11)61113-8)
- Zhu, H., & Stelson, K. A. (2003). Modeling and closed-loop control of stretch bending of aluminum rectangular tubes. *Journal of Manufacturing Science & Engineering*, 125(1), 113.
- Eggertsen, P. A., & Mattiassen, K. (2010). On constitutive modeling for springback analysis. *International Journal of Mechanical Sciences*, 52(6), 804–818.
- Dassault Systemes Simulia Corp (2014). Abaqus Analysis User's Manual 6.14; Dassault systemes simulia corp: Providence, RI, USA.
- Paulsen, F., & Welo, T. (2001). Cross-sectional deformations of rectangular hollow sections in bending: Part I—experiments. *International Journal of Mechanical Sciences*, 43(1), 109–129. [https://doi.org/10.1016/S0020-7403\(99\)00106-X](https://doi.org/10.1016/S0020-7403(99)00106-X)
- Li, G., Liu, Y., Du, T., & Tong, H. (2014). Algorithm research and system development on geometrical springback compensation system for advanced high-strength steel parts. *The International Journal of Advanced Manufacturing Technology*, 70(1–4), 413–427.

Publisher's Note Springer Nature remains neutral with regard to jurisdictional claims in published maps and institutional affiliations.



Song Gao Assistant professor, School of Mechatronic Engineering, ChangChun University of Technology. He received his undergraduate degree in Electronic Information Engineering at the Central South University (2009) and his Masters' degree and PhD in Vehicle Engineering from Dalian University of Technology (2015). Dr. Gao's research interests include 3D stretch-bending, Flexible forming, Advanced Manufacturer Technology and Plastic forming Technology for hard-

deformed materials.



Tonggui He Master student, School of Electrical and Mechanical Engineering, Changchun University of Technology, Major research fields include crystal plastic finite element simulation method and advanced manufacturing.



Yingli Sun Master Student, School of Mechatronic Engineering, ChangChun University of Technology. Major Research field is advanced flexible forming technology.



Jicai Liang Professor, College of Material Science and Engineering, Jilin University. His research focus on Advanced Manufacturer Technology and Plastic forming Technology.



Qihan Li professor, School of Mechatronic Engineering, Chang-Chun University of Technology. His research focus on Numerical simulation and process optimization of metal sheet plastic forming, mechanical clinching technology.